Photo-assisted electrochemical production of HClO and Fe^{2+} as Fenton-like reagents in chloride media for sulfamethoxazole degradation

María F. Murrieta [a], Enric Brillas [b], José L. Nava **[,a], Ignasi Sirés *[,b]

[a] *Departamento de Ingeniería Geomática e Hidráulica, Universidad de Guanajuato, Av. Juárez 77, Zona Centro, C.P 36000, Guanajuato, Guanajuato, Mexico*

[b] *Laboratori d'Electroquímica dels Materials i del Medi Ambient, Departament de Química Física, Facultat de Química, Universitat de Barcelona, Martí i Franquès 1-11, 08028 Barcelona, Spain*

Paper submitted to be published in *Separation and Purification Technology*

*Corresponding author: i.sires@ub.edu (I. Sirés)

** Corresponding author: jlnm@ugto.mx (J.L. Nava)

Abstract

The photoelectro-Fenton (PEF)-like process based on the replacement of H_2O_2 by HClO remains quite unexplored. Its ability to mineralize solutions containing 0.208 mM of the antibiotic sulfamethoxazole (SMX), either in 25 mM Na_2SO_4 + 35 mM NaCl or 45 mM Na_2SO_4 + 15 mM NaCl media, has been evaluated. The assays were performed in a 3 L pre-pilot flow plant composed of a filter-press FM01-LC reactor, which was equipped with an Ir-Sn-Ru oxide anode and a stainless steel cathode, coupled to an annular photoreactor containing a 160 W UVA lamp. A higher amount of active chlorine (HClO) was produced as the electrolysis was prolonged and the current density was increased. The accumulated HClO concentration dropped down more rapidly at a greater Fe^{2+} content due to the enhanced oxidant decomposition that yielded $^{\bullet}OH$ in the bulk. A continuous production of this radical was ensured from the effective Fe^{2+} regeneration, being favored by cathodic reduction and photoreduction of dissolved Fe(III) species. The SMX degradation was faster in 25 mM Na_2SO_4 + 35 mM NaCl mM because of the quicker HClO generation, although the larger proportion of recalcitrant chloro-derivatives and iron-chlorocomplexes decelerated the mineralization process. In 45 mM Na_2SO_4 + 15 mM NaCl, the best PEF-like treatment was attained at 0.4 mM Fe^{2+} and 15 mA cm^{-2}, achieving the complete antibiotic disappearance at 60 min and 59.7% mineralization after 420 min, with an energy consumption of 0.776 kWh $(g\ TOC)^{-1}$. Sixteen intermediates were detected by gas chromatography-mass spectroscopy, ten of which were chlorinated, allowing the proposal of a reaction route for SMX. Since the final solutions did not contain chloro-organics, the partial mineralization was mainly related to the accumulation of refractory non-chlorinated carboxylic acids that could not form photoactive Fe(III)-carboxylate complexes because of the presence of iron-chlorocomplexes.

Keywords: Active chlorine; Electrochemical oxidation; Hydroxyl radical; Pharmaceutical; Photoelectro-Fenton process; Wastewater treatment

1. Introduction

The increasing administration of drugs into human and animal bodies has caused a continuous discharge of unmetabolized residues into the aquatic environment [1]. The quality of natural and drinking water is thus severely affected, seriously jeopardizing our health [2.3]. Since conventional wastewater treatment plants (WWTPs) have demonstrated to be rather inefficient to remove pharmaceuticals from water [4,5], the investigation on more powerful methods is highly encouraged. As a result, novel technological approaches have been followed over the last decade, with positive impact on the removal of drugs and their metabolites or natural degradation by-products [4,6-9].

Sulfamethoxazole (SMX, 4-amino-*N*-(5-methyl-1,2-oxazol-3-yl)benzenesulfonamide, $C_{10}H_{11}N_3O_3S$, M = 253.279 g mol^{-1}) is a widely used antibiotic to treat bacterial infections, since it prevents the synthesis of folic acid in gram-positive and gram-negative bacteria. It is usually prescribed in conjunction with another antibiotic, trimethoprim, to treat urinary-tract infections [10]. However, about 15% of SMX in urine is in its parent form, reaching more than 20 μg L^{-1} in hospital wastewater, WWTPs and surface water [11,12]. Considering its prolonged half-life of 51.7 days in water [13], it is not surprising that its ecotoxicity has been well proven [13].

Electrochemical advanced oxidation processes (EAOPs) like electrochemical oxidation (EO), electro-Fenton (EF) and photoelectro-Fenton (PEF) have been utilized to degrade SMX. Their high oxidation power has been confirmed, which is attributed to the generation of strong oxidants like hydroxyl radical ($^{\bullet}OH$) and/or active chlorine [14-20]. The EO process has been studied either with a boron-doped diamond (BDD) anode in 20-100 mM K_2SO_4 at pH 4.0 [21] as well as in hospital wastewater [22], and with a dimensionally stable anode (DSA) like $Ti/Ru_{0.3}Ti_{0.7}O_2$ in 100 mM NaCl at pH 3.0 [23]. Overall SMX degradation but partial mineralization was always observed. Oturan and co-workers reported the total mineralization

of SMX solutions in pure sulfate medium at pH 3.0 by EF using a BDD/carbon-felt cell [24,25], as well as a 94% mineralization by heterogeneous EF with a Ti_4O_7 anode and a carbon-felt cathode modified with a $Fe^{II}Fe^{III}$ layered double hydroxide, also in pure sulfate medium [26]. The superiority of conventional PEF over EO and EF to remove up to 300 mg L^{-1} SMX has been described using a RuO_2/carbon fiber cell in sulfate medium [27], attaining 80% mineralization.

When the EO treatment is performed in the presence of Cl^-, the anode nature and the solution pH become key factors. Water oxidation at the anode M, which originates the strong physisorbed oxidant M(•OH) with E^o = 2.80 V/SHE via reaction (1), competes with Cl^- electro-oxidation to dissolved chlorine via reaction (2). This species, with $E°$ = 1.36 V/SHE, predominates at pH < 3.0, but it is converted to another active chlorine species like HClO ($E°$ = 1.49 V/SHE) at pH 3.0-8.0 via reaction (3) [18,19]. This gives rise to the so-called EO-HClO process [28]. BDD is the most powerful anode for M(•OH) production in sulfate medium, whereas active chlorine is predominant when a DSA is employed.

$$M + H_2O \rightarrow M(^{\bullet}OH) + H^+ + e^- \quad (1)$$

$$2Cl^- \rightarrow Cl_2(aq) + 2e^- \quad (2)$$

$$Cl_2(aq) + H_2O \rightarrow HClO + Cl^- + H^+ \quad (3)$$

The oxidation ability of the EO-HClO process can be enhanced by incorporating the relatively new concept of Fenton-like reaction (4), in which the production of the highly reactive oxidant •OH in the bulk solution is sustained by the continuous electrogeneration of HClO in the presence of Fe^{2+} at pH 2.8-3.5 [29-35]. In such EF-like treatment, Fe^{2+} can be slowly regenerated from cathodic reaction (5), thereby propagating the Fenton-like reaction (4) [36]. In a previous work [28], we explored the possibility of applying a PEF-like process to the destruction of Acid Red 1 azo dye. The mineralization was upgraded as compared to that

attained in the EF-like treatment, owing to the occurrence of photolytic reactions (6) and (7) [37]. Nonetheless, additional studies are required to confirm the positive features of the PEF-like process to degrade organic contaminants of emerging concern in Cl^- matrices.

$$HClO + Fe^{2+} \rightarrow Fe^{3+} + {}^{\bullet}OH + Cl^- \quad (4)$$

$$Fe^{3+} + e^- \rightarrow Fe^{2+} \quad (5)$$

$$Fe^{3+} + h\nu \rightarrow Fe^{2+} + {}^{\bullet}OH \quad (6)$$

$$Fe(OOCR)^{2+} + h\nu \rightarrow Fe^{2+} + CO_2 + R^{\bullet} \quad (7)$$

The aim of this work is to investigate, for the first time, the performance of PEF-like process regarding the removal of a pharmaceutical like SMX (EC_{50} = 1.57 mg L^{-1} for the green alga *Chloro vulgaris* [25]). The electrolyses were conducted in mixed sulfate + chloride media at pH 3.0, with different Fe^{2+} concentrations, using a flow plant equipped with an Ir-Sn-Ru oxide/stainless steel cell coupled to a UVA photoreactor. Comparative EO-HClO and EF-like trials clarified the role of the oxidizing agents and the UVA photons. The effect of applied current density (*j*) was also optimized examined. A degradation route for the electrochemical Fenton-like treatment of SMX was proposed, based on the main oxidation by-products detected by gas chromatography-mass spectrometry (GC-MS).

2. Materials and methods

2.1. Chemicals

Deionized water was employed to prepare the solutions to be electrolyzed, whereas ultrapure water was needed for the analysis of all samples. Sulfamethoxazole (98% purity) was purchased from Sigma-Aldrich. Analytical grade Na_2SO_4, NaCl and $FeSO_4 \cdot 7H_2O$ were supplied by Fluke, Merck and Panreac. The pH of SMX solutions was adjusted to 3.0 with analytical grade H_2SO_4 from Merck because this is the optimum value for water decontamination by

electrochemical Fenton-based processes [18,19]. Other chemicals were of either analytical or HPLC grade, either from Fluka, Merck, Panreac or Sigma-Aldrich.

2.2. Preparation of the Ir-Sn-Ru oxide anode

The ternary Ir-Sn-Ru oxide was synthesized on a Ti plate by means of the Pechini method following the same procedure described for an Ir-Sn-Sb oxide in our earlier work over [33]. The Sb-based oxide was replaced by Ru-based oxide to enhance the electrocatalytic activity and favor the accumulation of active chlorine, as well as to improve the stability of the Sn-based oxide in acidic medium [38]. Therefore, for the preparation of the electrode, $SbCl_3$ was replaced by $RuCl_3 \cdot xH_2O$. The whole coating comprised 32 layers, each one with the same molar proportion of metals (10% Ir, 63% Sn, 27% Ru). The electrode was finally heated at 550 ºC for 1 h.

2.3. Pre-pilot flow plant

The elements and connections of the pre-pilot flow plant have been described for other related EAOPs [39]. The reservoir was filled with 3.0 L of a given solution, which was then recirculated through the system at liquid flow rate of 180 L h^{-1} using a peristaltic pump. Two heat exchangers ensured a constant solution temperature of 30 ºC. The electrolytic cell was a filter-press FM01-LC reactor that contained the synthesized Ir-Sn-Ru oxide onto a Ti plate as the anode, a stainless steel plate as the cathode and a type-D turbulence promoter. The geometric area of both electrodes was 64 cm^2 (4 cm × 16 cm), with an interelectrode separation of 0.55 cm. In PEF-like process, a 160 W Omnilux 27E UVA lamp was placed inside an annular glass reactor with a capacity of 600 mL. The solution coming from the electrochemical reactor outlet was thus irradiated and sent back to the reservoir. The lamp was switched off in the EO-HCl and EF-like treatments. Constant current was provided by a Grelco GVD310 power supply, which simultaneously displayed the instantaneous cell voltage. Duplicated degradation trials were carried out with 0.208 mM SMX (25 mg L^{-1} of initial total organic carbon (TOC_0))

solutions, either in 25 mM Na_2SO_4 + 35 mM NaCl or 45 mM Na_2SO_4 + 15 mM NaCl, in the absence or presence of Fe^{2+}. These electrolyte concentrations were chosen because their conductivity was the same as that of a 50 mM Na_2SO_4 solution, typically employed by other authors and also used here to determine the reaction by-products.

2.4. Apparatus and analytical procedures

The solution pH was measured with a Crison 2000 pH meter. A 10% (v/v) NaOH solution was added to the samples immediately after collection to stop the degradation process, and each sample was filtered before its analysis. All the electrolytic trials were made twice and hence, the data shown in figures are accompanied by corresponding error bars. Active chlorine and Fe^{2+} contents were determined using standard colorimetric methods. A Shimadzu 1800 UV/Vis spectrophotometer was employed, set at λ = 515 nm [40] and λ = 510 nm, respectively [41].

Reversed-phase high-performance liquid chromatography (HPLC) allowed monitoring the SMX concentration decays. The measurements were carried with a Waters system composed of a 600 LC module and a 996 photodiode array detector (λ = 270 nm). The former was fitted with a BDS Hypersil C18, 250 mm × 4.6 mm (i.d.), column at 30 ºC. The sample volume injected was always of 20 µL, and the elution was achieved upon recirculation of a 70:30 (v/v) acetonitrile/water (10 mM KH_2PO_4, pH 3.0) mixture at 1.0 mL min^{-1}. A well-defined peak for the drug was obtained at a retention time of 7.5 min.

The Cl^- concentration was determined by ion chromatography with a Shimadzu system that included a conductivity detector. The sample volume injected was always of 25 µL. The anionic column was a Shim-Pack IC-A1S, 100 mm × 4.6 mm (i.d.) at 40 ºC, and the mobile phase was a solution containing 2.6 mM phthalic acid and 2.4 mM tris(hydroxymethyl)aminomethane) at pH 4.0 that was circulated at 1.5 L min^{-1}.

TOC removal ($\triangle(TOC)_{exp}$, in mg L^{-1}) was measured by injecting samples of 50 µL into a Shimadzu VCSN system [10]. The specific energy consumption per unit TOC mass (EC_{TOC}) at

159 a given time (*t*, in h) and applied current (*I*, in A), considering a solution volume (*V*, in L), was
160 calculated from Eq. (8) [18,19]. E_{cell} was the average cell voltage (in V), whose value was 4.7,
161 5.2 and 6.7 V at increasing *j* of 10, 15 and 25 mA cm^{-2}, respectively.

162 $$EC_{TOC}\ (kWh\ (g\ TOC)^{-1}) = \frac{E_{cell}\ I\ t}{V\ \triangle(TOC)_{exp}} \quad (8)$$

163 GC-MS allowed the determination of the main oxidation by-products formed after 30 and
164 120 min of electrolysis of solutions containing SMX either in 50 mM Na_2SO_4 or 45 mM Na_2SO_4
165 + 15 mM NaCl. An Agilent Technologies system was utilized following our previously
166 established procedure [42]. Non-polar Teknokroma Sapiens-X5ms and polar HP INNOWax
167 columns, both of 0.25 μm, 30 m × 0.25 mm (i.d.), were used.

168 **3. Results and discussion**

169 *3.1. Active chlorine generation under EO-HClO conditions in 25 mM Na_2SO_4 + 35 mM NaCl*

170 The treatment of SMX solutions was first assessed in a matrix containing 25 mM Na_2SO_4
171 + 35 mM NaCl at pH 3.0 and 30 ºC. Based on the relatively high Cl^- concentration, a large
172 production of active chlorine due to the great rate of reaction (2) could be hypothesized. To
173 clarify this assumption, the concentration of active chlorine over time during the electrolysis of
174 3 L of such mixed medium under EO-HClO conditions at different *j* values was determined.

175 Fig. 1 shows the increasing active chlorine (HClO as main species) content as the
176 electrolysis was prolonged for 240 min, at *j* from 5 to 20 mA cm^{-2}. In addition, a larger
177 accumulation was observed as the *j* value became higher. The lowest *j* (5 mA cm^{-2}) only yielded
178 1.22 mM of oxidant at the end of the electrolysis, which was drastically enhanced up to 5.9 and
179 16.8 mM at 10 and 15 mA cm^{-2}, respectively. Nonetheless, further increase of *j* to 20 mA cm^{-2}
180 had a less substantial effect on the accumulation, reaching about 18.5 mM. Considering the
181 Faraday's law, the efficiency of applied current to produce HClO was 15.3%, 37.1%, 70.0%

and 58.1% at increasing *j* values of 5, 10, 15 and 20 mA cm^{-2}, respectively. These findings allow concluding that 15 mA cm^{-2} was the best *j* referred to active chlorine production with the electrochemical reactor employed. This means that the applied current was partly invested in water oxidation to O_2, with the formation of the intermediate M(•OH) from reaction (1). From these results, the positive contribution of the synthesized DSA material is evident, but one could expect a better performance of PEF-like process thanks to the contribution of •OH formed in the bulk from reaction (4). This was evaluated at j = 15 mA cm^{-2}, as described below.

3.2. Treatment of SMX solutions by PEF-like process in 25 mM Na_2SO_4 + 35 mM NaCl

A solution with 0.208 mM SMX, corresponding to 25 mg L^{-1} of TOC, in 25 mM Na_2SO_4 + 35 mM NaCl at pH 3.0 and 30 ºC was first treated by EO-HClO (i.e., without Fe^{2+}). The concentration of the antibiotic decayed rapidly, with total disappearance at 25 min, as depicted in Fig. 2a. This rapid abatement obeyed a pseudo-first-order reaction kinetics (see inset of Fig. 2a) and can be ascribed to the attack of a steady concentration of generated oxidants like M(•OH) and, especially, active chlorine from reactions (1)-(3). An apparent rate constant (k_1) of 0.15 min^{-1}, with R^2 = 0.987, was obtained for SMX removal in this process. In contrast to its fast degradation, Fig. 2b reveals a much slower mineralization of 33.1% for the first 60 min of electrolysis, whereupon the TOC removal was even slower and finally attained 38% at 150 min. The partial mineralization achieved in EO-HClO process can be plausibly attributed to the large generation of chloro-derivatives, which are known to be very stable against M(•OH) and chlorine [18,19].

Solutions with an analogous composition in the presence of Fe^{2+} were then treated under PEF-like conditions. The SMX removal was improved because oxidant •OH was simultaneously produced from reaction (4). The continuous regeneration of Fe^{2+} from reactions (5) and (6) allowed maintaining the rate of reaction (4) and, as a result, the mixture of oxidizing agents (M(•OH), •OH and active chlorine) upgraded the decontamination. Fig. 2a shows that,

0.4 mM Fe^{2+}, the antibiotic was completely degraded in only 20 min. From the good linear profiles obtained when a pseudo-first-order reaction kinetics was considered (see inset), a k_1-value of 0.23 min^{-1}, i.e., 1.5-fold higher than that mentioned for EO-HClO, was found. This can be justified by an effective production of $^{\bullet}OH$, not only via reaction (4) but also via reaction (6), which eventually makes the PEF-like process much more powerful than EO-HClO. Conversely, Fig. 2a highlights a clear inhibition of SMX removal when the Fe^{2+} concentration was increased to 0.5 mM. In this case, the time for the complete antibiotic disappearance was larger, requiring 30 min, resulting in a lower k_1-value as compared to that using 0.4 mM Fe^{2+} (see Table 1). This phenomenon suggests a drastic restriction of the amounts of oxidizing agents available at 0.5 mM Fe^{2+}, which can be explained by: (i) the partial loss of HClO, which is an effective oxidant to degrade the antibiotic, owing to its decomposition via reaction (4); and (ii) the faster destruction of generated $^{\bullet}OH$ from side events like its dimerization reaction (9). Note that an excessive amount of this radical can also partly consume the generated H_2O_2 via reaction (10) and the excess of Fe^{2+} to yield the weaker oxidant hydroperoxyl radical ($HO_2^{\bullet}$) via reaction (11) [37,43].

$$2^{\bullet}OH \rightarrow H_2O_2 \quad (9)$$

$$H_2O_2 + {}^{\bullet}OH \rightarrow HO_2^{\bullet} + H_2O \quad (10)$$

$$Fe^{2+} + {}^{\bullet}OH \rightarrow Fe^{3+} + OH^- \quad (11)$$

According to the above behavior, Fig. 2b highlights the low TOC abatement achieved under PEF-like conditions. The quickest mineralization was found during the first 60 min of treatment, leading to 37.2% and 16.7% TOC removal using 0.4 and 0.5 mM Fe^{2+}, respectively. These values could not be significantly improved thereafter, as can be seen in Table 1. This table also shows the smallest EC_{TOC} value operating with 0.4 mM Fe^{2+} due to the larger TOC reduction. The low mineralization achieved in the PEF-like process might be related again with

231 the production of recalcitrant chloro-derivatives, behaving as quite photostable substances
232 under UVA illumination. Moreover, the formation of a large amount of Fe(III)-carboxylate
233 species, which could easily undergo photodecomposition via reaction (7), can be discarded as
234 well because in a medium with that high Cl^- concentration the iron ions tend to form ferrous-
235 and ferric-chlorocomplexes like $FeCl^+$, $FeCl^{2+}$ and $FeCl_2^+$ [44,45]. This inhibits the formation
236 of sufficient amounts of Fe(III)-carboxylate complexes, thereby impeding a more quantitative
237 mineralization because the uncomplexed short-chain carboxylic acids are very resistant to •OH
238 [14]. All these findings indicate that the use of too high Cl^- contents is detrimental for the
239 mineralization of the antibiotic. For this reason, in the next subsections the PEF-like process
240 was assessed in the presence of less chloride but keeping the same conductivity [28,33].

241 *3.3. Active chlorine generation and Fe^{2+} evolution under PEF-like conditions in 45 mM Na_2SO_4*
242 *+ 15 mM NaCl*

243 The influence of Fe^{2+} content on active chlorine generation was examined to confirm the
244 contribution of the Fenton-like reaction (4) in the PEF-like process in 45 mM Na_2SO_4 + 15 mM
245 NaCl at pH 3.0 and 30 ºC. Fig. 3 depicts the continuous accumulation of active chlorine up to
246 1.86 mM at 120 min in EO-HClO at j = 15 mA cm^{-2}. This corresponds to a current efficiency
247 of 15.6%, which contrasts with 55.0% at 120 min (i.e., 6.56 mM) determined in 25 mM Na_2SO_4
248 + 35 mM NaCl (Fig. 1). This is an evidence of the direct dependence of the rate of reaction (2)
249 on the chloride concentration in the mixed electrolyte. Consequently, the low Cl^- content in the
250 new medium is expected to accelerate the anodic water discharge, ending in a higher production
251 of M(•OH) from reaction (1).

252 Fig. 3 also shows a progressive decrease in the final active chlorine accumulation, from
253 1.58 to 0.89 mM, as the Fe^{2+} content was increased from 0.3 to 2.0 mM under PEF-like
254 conditions. This phenomenon can be accounted for by the quicker decomposition rate of HClO
255 via reaction (4) stimulated by the larger catalyst content. In all these PEF-like trials, the HClO

256 production was accompanied by a Cl^- decay of about 2.3-2.6 mM. Note that, as commented
257 above, an excess of •OH can be detrimental depending on the relative rate of its parasitic
258 reactions (9)-(11).

259 The Fe^{2+} evolution during the treatments carried out in the same medium was also
260 investigated. A preliminary EF-like trial (i.e., without UVA illumination) was made in the
261 presence of 0.3 mM Fe^{2+}, at j = 15 mA cm^{-2}. Fig. 4a shows a decay of the initial catalyst
262 concentration down to a steady value of 0.20 mM, which was attained once its oxidation rate
263 via reaction (4) became equal to its regeneration rate via reaction (5) at the stainless steel
264 cathode surface. This situation became different applying the PEF-like process under UVA
265 irradiation. It is noticeable from Fig. 4b that a steady state for Fe^{2+} concentration could be
266 reached at starting Fe^{2+} contents of 0.3 and 0.5 mM. At 0.3 mM, the steady value was 0.24 mM,
267 which was higher than that obtained in EF-like process. The increase can be explained by the
268 simultaneous regeneration of this ion via photo-Fenton reaction (6). This should presumably
269 result in a greater generation of oxidant •OH from reactions (4) and (6), making the PEF-like
270 process more powerful than the EF-like one. Fig. 4b also evidences a gradual decrease of the
271 normalized Fe^{2+} content as its initial load became higher, which agrees with the lower HClO
272 accumulation shown in Fig. 3. However, the curves at 1.0 and 2.0 mM Fe^{2+} in Fig 4b did not
273 reach a plateau, which means that the progressively higher rate of reaction (4) could not be
274 counterbalanced by the rate of reactions (5) and (6). One can thus deduce that a range of 0.3-
275 0.5 mM Fe^{2+} is suitable to operate the PEF-like process with a continuous and steady (i.e., well
276 controlled) production of oxidizing agents.

277 *3.4. PEF-like treatment of SMX solutions in 45 mM Na_2SO_4 + 15 mM NaCl*

278 The degradation and mineralization of 0.208 mM SMX in 45 mM Na_2SO_4 + 15 mM NaCl
279 with 0.4 mM Fe^{2+} at pH 3.0 and 30 ºC by the PEF-like process was first studied at different j
280 values ranging between 10 and 25 mA cm^{-2}. This operation parameter is crucial to regulate the

rate of the electrode reactions, which modulate the production of oxidizing agents as discussed before. Fig. 5a depicts that the antibiotic decay was accelerated at higher *j*, disappearing after 110, 60 and 50 min at 10, 15 and 25 mA cm^{-2}, respectively. This enhancement arises from the gradual increase in rate of reactions (1), (2), (4) and (5), alongside the indirect positive impact on reaction (6) because of the generation of more Fe(III) species. This led to the formation of larger quantities of M(•OH), •OH and active chlorine that could attack SMX and its by-products. The inset of Fig. 5a corroborates the pseudo-first reaction order for the SMX abatement in these assays, suggesting its reaction with a growing steady concentration of oxidants. Table 1 shows that the k_1-value was 3.4-fold greater when *j* rose 2.5 times, from 10 to 25 mA cm^{-2}. Therefore, the UVA light was clearly synergistic, leading to larger enhancement of •OH production than the expected from the electrical consumption, increasing the viability of the process.

However, Fig. 5b illustrates a low TOC abatement for 420 min under the above conditions. The mineralization was upgraded when *j* was increased from 10 to 15 mA cm^{-2}, attaining a final TOC reduction of 44.5% and 59.7%, respectively. Conversely, at the highest *j* of 25 mA cm^{-2}, the mineralization process was decelerated, yielding a much poorer TOC removal (see Table 1). As in the case of trials performed in 25 mM Na_2SO_4 + 35 mM NaCl, one can infer either the formation of a substantial amount of recalcitrant chloro-derivatives even in this new medium with a lower Cl^- content or, more plausibly, the predominance of iron-chlorocomplexes mentioned in sub-section 3.2 over the photoactive Fe(III)-carboxylate complexes. The loss of oxidation power at 25 mA cm^{-2} can be associated with the lower availability of •OH, caused by the greater extent of parasitic reactions (9)-(11), along with the faster anodic oxidation of HClO to undesirable ClO_3^- and ClO_4^- ions that are not effective to oxidize the organics [28,39]. A value of 15 mA cm^{-2} was then established as the best *j*, as also confirmed by the corresponding EC_{TOC} value (see Table 1).

The influence of Fe^{2+} concentration between 0.3 and 1.0 mM on the performance of the PEF-like treatment of 0.208 mM SMX in 45 mM Na_2SO_4 + 15 mM NaCl at pH 3.0 and 30 ºC was finally examined at the optimized *j* of 15 mA cm^{-2}. As can be observed in Fig. 6a, the antibiotic was removed at a similar rate using 0.3 and 0.4 mM Fe^{2+}, achieving its total disappearance at 60 min. A slower abatement was observed at higher catalyst contents, requiring 90 min at 1.0 mM Fe^{2+}. In these assays, steady but gradually decreasing amounts of oxidizing agents reacted with SMX, as inferred from the good linear correlations with a decreasing slope (inset of Fig. 6a) when a pseudo-first-order kinetic analysis was made. Table 1 shows a similar k_1-value in trials with 0.3 and 0.4 mM Fe^{2+}, with a 0.4-fold decay at 1.0 mM Fe^{2+}. This tendency could seem opposite to the clear enhancement of the HClO decomposition as the Fe^{2+} concentration was increased, as described from Fig. 3 and 4. Hence, this confirms the acceleration of reactions (9)-(11) that caused a gradual loss of oxidant •OH, negatively affecting the antibiotic destruction. This phenomenon can also be observed from the TOC-time profiles shown in Fig. 6b. The highest mineralization was achieved at 0.4 mM Fe^{2+}, being superior to that attained at 0.3 and 0.5 mM Fe^{2+}. A TOC reduction of 59.7% was achieved, resulting in the lowest EC_{TOC} value of 0.776 kWh (g TOC)$^{-1}$ (see Table 1). The best performance of the PEF-like treatment in 45 mM Na_2SO_4 + 15 mM NaCl at pH 3.0 was then found at 0.4 mM Fe^{2+} and *j* = 15 mA cm^{-2}, thus confirming the results highlighted in 25 mM Na_2SO_4 + 35 mM NaCl. It is interesting to note that the k_1-value in this latter medium was 5.2-fold higher than that in the former one when the best operation conditions were compared (see Table 1). This is related to the greater production of active chlorine, which reacted more rapidly with SMX. However, the attack of such higher quantities of HClO originated a larger proportion of chloro-derivatives, ending in a lower TOC removal (41.0% vs ~50% at 150 min, see Table 1 and Fig. 6b). That means that the decrease of Cl^- in the aqueous matrix favors the mineralization of chloro-organics, especially by •OH.

330 *3.5. Proposed route for SMX degradation*

331 The by-products formed after 30 and 120 min of PEF-like treatment of 0.208 mM SMX in
332 45 mM Na_2SO_4 + 15 mM NaCl with 0.4 mM Fe^{2+} at pH 3.0 and 15 mA cm^{-2} were detected by
333 GC-MS. This analysis was also made by the EO-HClO in 50 mM Na_2SO_4 under the same
334 conditions to better clarify the by-products only formed from the attack of hydroxyl radicals.
335 These results revealed the generation of sixteen compounds that included four aromatic and two
336 heterocyclic non-chlorinated intermediates, along with five aromatic monochloro-derivatives,
337 three aromatic dichloro-derivatives, one linear dichloro-derivative and one linear trichloro-
338 derivative. Worth remarking, no chlorinated organic compounds were detected at 420 min.
339 Based on the detected by-products, a degradation route for SMX (**1**) is proposed in Fig. 7. It is
340 presupposed that hydroxyl radicals (generalized as •OH) and active chlorine (HClO) were the
341 main oxidants, and the *m/z* values of chlorinated compounds were determined on the basis of
342 the isotope ^{35}Cl.

343 The pathway is initiated by the cleavage of either the N-S bond linked to the oxazol-3-yl
344 group of **1** or its N-C bond to yield *N*-(5-methylisoxazol-3-yl)acetamide (**2**, *m/z* 125) after
345 reaction with some linear hydrocarbon or 4-aminobenzenesulfonamide (**3**, *m/z* 172),
346 respectively. Decarbonylation of compound **2** then gives 5-methylisoxazolamine (**4**, *m/z* 98),
347 which is degraded and consecutive chlorinated to produce 2,2-dichlorocetamide (**5**, *m/z* 127)
348 and 2,2,2-trichloroacetamide (**6**, *m/z* 161). Worth noting, the cleavage of **1** and **2** can be
349 attributed to the action of •OH, although this type of rupture may also be induced by HClO
350 without any simultaneous chlorination, simply because of its high redox potential. This can
351 partly explain the large enhancement of k_1-value with increasing NaCl content (see Table 1).
352 On the other hand, compound **3** is transformed into 4-aminobenzenethiol (**7**, *m/z* 125), which
353 can be either hydroxylated to form aniline (**8**, *m/z* 93) or chlorinated to originate a mixture of
354 4-chloroaniline (**12**, *m/z* 127) and 2-chloroaniline (**13**, *m/z* 127). Further hydroxylation of

compound **8** leads to hydroquinone (**9**, *m/z* 110). This compound undergoes two consecutive chlorination steps to yield 2-chloro-1,4-benzenediol (**10**, *m/z* 144) and 2,5-dichloro-1,4-benzenediol (**11**, *m/z* 178). Hydroxylation of the mixture of **12** + **13** can cause deamination to give a mixture of 4-chlorophenol (**14**, *m/z* 128) and 2-chlorophenol (**15**, *m/z* 128). Chlorination of the mixtures of **12** + **13** and **14** + **15** finally yields 2,4-dichloroaniline (**16**, *m/z* 161) and 2,4-dichlorophenol (**17**, *m/z* 162), respectively, whereas the deamination of compound **16** can also produce **17**. Note that the three aminochloro-derivatives (**12**, **13** and **16**) can also be degraded to **5** and/or **6**. Moreover, the hydroxylation of compounds **14** and **15** can lead to compounds **9** and **10**, respectively. Since, as stated above, chloroorganics were not accumulated in the solutions electrolyzed for 420 min, it can be inferred that the most plausible reason to explain the plateau reached in TOC-time plots in this medium (Fig. 5b and Fig. 6b) was the entrapment of iron catalyst in iron-chlorocomplexes (see sub-sections 3.2 and 3.4). Hence, the carboxylic acids expected to be generated from the intermediates of Fig. 7 [25] could not form photoactive Fe(III)-carboxylate complexes, thus remaining as very persistent uncomplexed acids. In addition, the high number of chloro-derivatives detected during the PEF-like treatment of SMX accounted for the low mineralization rate before reaching the plateau.

4. Conclusions

The singular PEF-like process with HClO playing the role of H_2O_2 and UVA photons allowing the Fe^{2+} regeneration was able to completely remove SMX from sulfate + chloride matrices at pH 3.0 using a flow electrochemical reactor. The antibiotic was more rapidly abated in the presence of a greater NaCl concentration (35 mM vs. 15 mM) due to the faster attack of active chlorine electrogenerated. Conversely, a larger mineralization occurred when the chloride content was diminished because of the enhanced production of reactive $^{\bullet}OH$. The parasitic reactions that destroyed this radical became more relevant when the Fe^{2+} content was

increased, despite causing a quicker HClO decomposition, eventually hampering the degradation and mineralization of the antibiotic. The same phenomenon was observed with increasing *j* from 15 to 25 mA cm^{-2}. Under the best conditions in 45 mM Na_2SO_4 + 15 mM NaCl (i.e., 0.4 mM Fe^{2+} and *j*= 15 mA cm^{-2}), SMX was completely removed in 60 min, achieving 59.7% mineralization after 420 min of electrolysis. A degradation route for the antibiotic by electrochemical Fenton-like treatments has been proposed considering the sixteen compounds detected by GC-MS. The appearance of chloro-derivatives and, more important, the accumulation of final recalcitrant products like carboxylic acids in their uncomplexed form allows explaining the partial mineralization of SMX solutions by PEF-like process. The addition of more Fe^{2+} catalyst once reached the mineralization plateau could break the inhibition caused by the iron-chlorocomplexes. Alternatively, a less expensive biological post-treatment could also improve the mineralization because of the absence of toxic chloro-organics.

Acknowledgements

The authors sincerely acknowledge the financial support from projects CTQ2016-78616-R (AEI/FEDER, EU) and No. 102/2019 (Universidad de Guanajuato, Mexico). M.F. Murrieta thanks CONACYT (Mexico) for her PhD scholarship No. 786726.

References

[1] M. Mezzelani, S. Gorbi, F. Regoli, Pharmaceuticals in the aquatic environments: Evidence of emerged threat and future challenges for marine organisms, Mar. Environ. Res. 140 (2018) 41-60. doi.org/10.1016/j.marenvres.2018.05.001

[2] M. Ashfaq, Y. Li, M.S.U. Rehman, M. Zubair, G. Mustafa, M.F. Nazar, C.-P. Yu, Q. Sun Q, Occurrence, spatial variation and risk assessment of pharmaceuticals and personal care

products in urban wastewater, canal surface water, and their sediments: a case study of Lahore, Pakistan, Sci. Total Environ. 688 (2019) 653-663. doi.org/10.1016/j.scitotenv.2019.06.285

[3] I.Y. López-Pacheco, A. Silva-Narváez, C. Salinas-Salazar, A. Arévalo-Gallegos, L.A. Lizarazo-Holguin, D. Barceló, H.M.N. Iqbal, R. Parra-Saldívar, Anthropogenic contaminants of high concern: existence in water resources and their adverse effects, Sci. Total Environ. 690 (2019) 1068-1088. doi.org/10.1016/j.scitotenv.2019.07.052

[4] Y. Luo, W. Guo, H.H. Ngo, L.D. Nghiem, F.I. Hai, J. Zhang, S. Liang, X.C. Wang, A review on the occurrence of micropollutants in the aquatic environment and their fate and removal during wastewater treatment, Sci. Total Environ. 473-474 (2014) 619-641. doi.org/10.1016/j.scitotenv.2013.12.065

[5] L.A. Schaider, K.M. Rodgers, R.A. Rudel, Review of organic wastewater compound concentrations and removal in onsite wastewater treatment systems, Environ. Sci. Technol. 51 (2017) 7304-7317. doi.org/10.1021/acs.est.6b04778

[6] I. Sirés, E. Brillas, Remediation of water pollution caused by pharmaceutical residues based on electrochemical separation and degradation technologies: a review, Environ. Int. 40 (2012) 212-229. doi.org/10.1016/j.envint.2011.07.012

[7] J. Rivera-Utrilla, M. Sánchez-Polo, M.O. Ferro-García, G. Prados-Joya, R. Ocampo-Pérez, Pharmaceuticals as emerging contaminants and their removal from water. A review, Chemosphere 93 (2013) 1268-1287. doi.org/10.1016/j.chemosphere.2013.07.059

[8] E. Brillas, I. Sirés, Electrochemical removal of pharmaceuticals from water streams: reactivity elucidation by mass spectrometry, TrAC–Trend Anal. Chem. 70 (2015) 112-121. doi.org/10.1016/j.trac.2015.01.013

425 [9] D. Kanakaraju, D.D. Glass, M. Oelgemöller, Advanced oxidation process-mediated
426 removal of pharmaceuticals from water: a review, J. Environ. Manage. 219 (2018) 89-
427 207. doi.org/10.1016/j.jenvman.2018.04.103
428 [10] J.C. Murillo-Sierra, I. Sirés, E. Brillas, E.J. Ruiz-Ruiz, A. Hernández-Ramírez, Advanced
429 oxidation of real sulfamethoxazole trimethoprim formulations using different anodes and
430 electrolytes, Chemosphere 192 (2018) 225-233.
431 doi.org/10.1016/j.chemosphere.2017.10.136
432 [11] H. Singer, S. Jaus, I. Hanke, A. Luck, J. Hollender, A.C. Alder, Determination of biocides
433 and pesticides by on-line solid phase extraction coupled with mass spectrometry and their
434 behaviour in wastewater and surface water, Environ Pollut. 158 (2010) 3054-3064.
435 doi.org/10.1016/j.envpol.2010.06.013
436 [12] A.N. Ngigi, M.M. Magu, B.M. Muendo, Occurrence of antibiotics residues in hospital
437 wastewater, wastewater treatment plant, and in surface water in Nairobi County, Kenya,
438 Environ. Monit. Assess. 192 (2020) 18. doi.org/10.1007/s10661-019-7952-8
439 [13] G. Prasannamedha, P. Senthil Kumar, A review on contamination and removal of
440 sulfamethoxazole from aqueous solution using cleaner techniques: present and future
441 perspective, J. Clean. Prod. 250 (2020) 119553. doi.org/10.1016/j.jclepro.2019.119553
442 [14] E. Brillas, I. Sirés, M.A. Oturan, Electro-Fenton process and related electrochemical
443 technologies based on Fenton's reaction chemistry, Chem. Rev. 109 (2009) 6570-6631.
444 doi.org/10.1021/cr900136g
445 [15] E. Brillas, A review on the degradation of organic pollutants in waters by UV
446 photoelectro-Fenton and solar photoelectro-Fenton, J. Braz. Chem. Soc. 25 (2014) 393-
447 417. doi.org/10.5935/0103-5053.20130257
448 [16] S. Vasudevan, M.A. Oturan, Electrochemistry as cause and cure in water pollution. An
449 overview, Environ. Chem. Lett. 12 (2014) 97-108. doi.org/10.1007/s10311-013-0434-2

[17] M.A. Oturan, J.-J. Aaron, Advanced oxidation processes in water/wastewater treatment: principles and applications. a review, Crit. Rev. Environ. Sci. Technol. 44 (2014) 2577-2641. doi.org/10.1080/10643389.2013.829765

[18] C.A. Martínez-Huitle, M.A. Rodrigo, I. Sirés, O. Scialdone, Single and coupled electrochemical processes and reactors for the abatement of organic pollutants: a critical review, Chem. Rev. 115 (2015) 13362-13407. doi.org/10.1021/acs.chemrev.5b00361

[19] F.C. Moreira, R.A.R. Boaventura, E. Brillas, V.J.P. Vilar, Electrochemical advanced oxidation processes: a review on their application to synthetic and real wastewaters, Appl. Catal. B: Environ. 202 (2017) 217-261. doi.org/10.1016/j.apcatb.2016.08.037

[20] X. Liu, Y. Zhou, J. Zhang, L. Luo, Y. Yang, H. Huang, H. Peng, L. Tang, Y. Mu, Insight into electro-Fenton and photo-Fenton for the degradation of antibiotics: mechanism study and research gaps, Chem. Eng. J. 347 (2018) 379-397. doi.org/10.1016/j.cej.2018.04.142

[21] Y. Lan, C. Coetsier, C. Causserand, K. Groenen-Serrano, An experimental and modelling study of the electrochemical oxidation of pharmaceuticals using a boron-doped diamond anode, Chem. Eng. J. 333 (2018) 486-494. doi.org/10.1016/j.cej.2017.09.164

[22] G. Loos, T. Scheers, K. Van Eyck, A. Van Schepdael, E. Adams, B. Van der Bruggen, D. Cabooter, R, Dewil, Electrochemical oxidation of key pharmaceuticals using a boron doped diamond electrode, Sep. Purif. Technol. 195 (2018) 184-191. doi.org/10.1016/j.seppur.2017.12.009

[23] S. Hussain, S. Gul, J.R. Steter, D.W. Miwa, A.J. Motheo, Route of electrochemical oxidation of the antibiotic sulfamethoxazole on a mixed oxide anode, Environ. Sci. Pollut. Res. 22 (2015) 15004-15015. doi.org/10.1007/s11356-015-4699-9

[24] A. Dirany, I. Sirés, N. Oturan, M.A. Oturan, Electrochemical abatement of the antibiotic sulfamethoxazole from water, Chemosphere 81 (2010) 594–602. doi.org/10.1016/j.chemosphere.2010.08.032

[25] A. Dirany, S. Efremova Aaron, N. Oturan, I. Sirés, M.A. Oturan, J.J. Aaron, Study of the toxicity of sulfamethoxazole and its degradation products in water by a bioluminescence method during application of the electro-Fenton treatment, Anal. Bioanal. Chem. 400 (2011) 353-360. doi.org/10.1007/s00216-010-4441-x

[26] S.O. Ganiyu, T.X.H. Le, M. Bechelany, N. Oturan, S. Papirio, G. Esposito, E. van Hullebusch, M. Cretin, M.A. Oturan, Electrochemical mineralization of sulfamethoxazole over wide pH range using $Fe^{II}Fe^{III}$ LDH modified carbon felt cathode: degradation pathway, toxicity and reusability of the modified cathode, Chem. Eng. J. 350 (2018) 844-855. doi.org/10.1016/j.cej.2018.04.141

[27] A. Wang, Y.-Y. Li, A.L. Estrada, Mineralization of antibiotic sulfamethoxazole by photoelectro-Fenton treatment using activated carbon fiber cathode and under UVA irradiation, Appl. Catal. B: Environ. 102 (2011) 378-386. doi.org/10.1016/j.apcatb.2010.12.007

[28] M.F. Murrieta, I. Sirés, E. Brillas, J.L. Nava, Mineralization of Acid Red 1 azo dye by solar photoelectro-Fenton-like process using electrogenerated HClO and photoregenerated Fe(II), Chemosphere 246 (2020) 125697. doi.org/10.1016/j.chemosphere.2019.125697

[29] L.P. Candeias, M.R.L. Stratford, P. Wardman, Formation of hydroxyl radicals on reaction of hypochlorous acid with ferrocyanide, a model iron (II) complex, Free Radic. Res. 20 (1994) 241-249. doi.org/10.3109/10715769409147520

[30] N. Kishimoto, E. Sugimura, Feasibility of an electrochemically assisted Fenton method using Fe^{2+}/HOCl system as an advanced oxidation process, Water Sci. Technol. 62 (2010) 2321-2329. doi.org/10.2166/wat.2010.203

[31] N. Kishimoto, T. Kitamura, M. Kato, H. Otsu, Influence of chelating agents on Fenton-type reaction using ferrous ion and hypochlorous acid, J. Water Environ. Technol. 11 (2013) 21-32. doi.org/10.2965/jwet.2013.21

[32] J. Behin, A. Akbari, M. Mahmoudi, M. Khajeh, Sodium hypochlorite as an alternative to hydrogen peroxide in Fenton process for industrial scale, Water Res. 121 (2017) 120-128. dx.doi.org/10.1016/j.watres.2017.05.015

[33] Z.G. Aguilar, E. Brillas, M. Salazar, J.L. Nava, I. Sirés, Evidence of Fenton-like reaction with active chlorine during the electrocatalytic oxidation of Acid Yellow 36 azo dye with Ir-Sn-Sb oxide anode in the presence of iron ion, Appl. Catal. B: Environ. 206 (2017) 44-52. doi.org/10.1016/j.apcatb.2017.01.006

[34] D.A.C. Coledan, I. Sánchez-Montes, B.F. Silva, J.M. Aquino, On the performance of HOCl/Fe^{2+}, HOCl/Fe^{2+}/UVA, and HOCl/UVC processes using in situ electrogenerated active chlorine to mineralize the herbicide picloram, Appl. Catal. B: Environ. 227 (2018) 170-177. doi.org/10.1016/j.apcatb.2017.12.072

[35] S. Liang, L, Zhu, J. Hua, W. Duan, P.-T. Yang, S.-L. Wang, C. Wei, C. Liu, C. Feng, Fe^{2+}/HClO reaction produces $Fe^{IV}O^{2+}$: an enhanced advanced oxidation process, Environ. Sci. Technol. (2020). doi.org/10.1021/acs.est.0c00218

[36] M. Panizza, M.A. Oturan, Degradation of Alizarin Red by electro-Fenton process using a graphite-felt cathode, Electrochim. Acta 56 (2011) 7084-7087. doi.org/10.1016/j.electacta.2011.05.105

[37] J. Steter, E. Brillas, I. Sirés, On the selection of the anode material for the electrochemical removal of methylparaben from different aqueous media, Electrochim. Acta 222 (2016) 1464-1474. doi.org/10.1016/j.electacta.2016.11.125

[38] A.I. Onouchukwu, S. Trasatti, Effect of substitution of SnO_2 for TiO_2 on the surface and electrocatalytic properties of RuO_2 + TiO_2 electrodes, J. Appl. Electrochem. 21 (1991) 858-862. doi.org/10.1007/BF01042451

[39] A. Thiam, R. Salazar, E. Brillas, I. Sirés, Electrochemical advanced oxidation of carbofuran in aqueous sulfate and/or chloride media using a flow cell with a RuO_2-based anode and an air-diffusion cathode at pre-pilot scale, Chem. Eng. J. 335 (2018) 133-134. doi.org/10.1016/j.cej.2017.10.137

[40] APWA, AWWA, WEF, Standard Methods for the Examination of Water and Wastewater, 21st Ed. Method number 4500 - Cl Chlorine (residual) – G. DPD colorimetric method, American Public Health Association, Washington D.C, USA, 2005. pp. 4-67–4-68.

[41] AWWA, AWWA, WEF, Standard Methods for the Examination of Water and Wastewater, 21st Ed. Fe^{2+} content from the red complex formed with 1,10-phenanthroline, American Public Health Association, Washington D.C, USA, 2005. pp. 3-77–3-79.

[42] G. Coria, T. Pérez, I. Sirés, E. Brillas, J.L. Nava, Abatement of the antibiotic levofloxacin in a solar photoelectro-Fenton flow plant: modeling the dissolved organic carbon concentration-time relationship, Chemosphere 198 (2018) 174-181. doi.org/10.1016/j.chemosphere.2018.01.112

[43] S. Lanzalaco, I. Sirés, M.A. Sabatino, C. Dispenza, O. Scialdone, A. Galia, Synthesis of polymer nanogels by electro-Fenton process: investigation of the effect of main operation parameters, Electrochim. Acta 246 (2017) 812-822. doi.org/10.1016/j.electacta.2017.06.097

[44] M.-C. Lu, Y.-F. Chang, I.-M. Chen, Y.-Y. Huang, Effect of chloride ions on the oxidation of aniline by Fenton's reagent, J. Environ. Manage. 75 (2005) 177-182. doi:10.1016/j.jenvman.2004.12.003

[45] J. De Laat, T.G. Le, Effects of chloride ions on the iron(III)-catalyzed decomposition of hydrogen peroxide and on the efficiency of the Fenton-like oxidation process. Appl. Catal. B: Environ. 66 (2006) 137-146. doi:10.1016/j.apcatb.2006.03.008

551 **Figure captions**

552 **Fig. 1.** Influence of current density on the concentration of active chlorine vs. treatment time
553 for the electrolysis of 3.0 L of 25 mM Na_2SO_4 + 35 mM NaCl solutions at pH 3.0 and 30 ºC,
554 using a filter-press FM01-LC flow reactor with an Ir-Sn-Ru oxide anode and a stainless steel
555 cathode, both of 64 cm^2 area, at liquid flow rate of 180 L h^{-1}.

556 **Fig. 2.** Change of normalized (a) SMX and (b) TOC concentrations with electrolysis time
557 during the treatment of 3.0 L of 0.208 mM antibiotic (25 mg L^{-1} TOC_0) solutions with 25 mM
558 Na_2SO_4 + 35 mM NaCl at pH 3.0 and 30 ºC, using the same reactor described in Fig. 1 at 15
559 mA cm^{-2} and 180 L h^{-1}. Method: EO-HClO (without Fe^{2+}); and PEF-like with 0.4 and 0.5 mM
560 Fe^{2+} and a 160 W UVA lamp. In (a), the pseudo-first-order kinetic analysis of SMX
561 concentration decays is shown in the inset panel.

562 **Fig. 3.** Time course of active chlorine concentration during the EO-HClO (without Fe^{2+}) and
563 PEF-like (at different Fe^{2+} contents with a 160 W UVA lamp) treatment of 3.0 L of 45 mM
564 Na_2SO_4 + 15 mM NaCl solutions at pH 3.0 and 30 ºC, using the same reactor described in Fig.
565 1 at 15 mA cm^{-2} and 180 L h^{-1}.

566 **Fig. 4.** Time course of the normalized Fe^{2+} concentration during the treatment of 3.0 L of 0.208
567 mM SMX solutions with 45 mM Na_2SO_4 + 15 mM NaCl at pH 3.0 and 30 ºC, using the same
568 reactor described in Fig. 1 at 15 mA cm^{-2} and 180 L h^{-1}. Method: (a) EF-like with 0.3 mM Fe^{2+}
569 and (b) PEF-like at the same Fe^{2+} contents shown in Fig. 3.

570 **Fig. 5.** Influence of current density on the variation of normalized (a) SMX and (b) TOC
571 concentrations with electrolysis time for the PEF-like treatment of 3.0 L of 0.208 mM antibiotic
572 solutions with 45 mM Na_2SO_4 + 15 mM NaCl and 0.4 mM Fe^{2+} at pH 3.0 and 30 ºC, maintaining
573 the other conditions described in Fig. 4. The inset panel of (a) presents the pseudo-first-order
574 kinetic analysis of SMX concentration removals.

575 **Fig. 6.** Effect of initial Fe^{2+} concentration on the time course of normalized (a) SMX
576 concentration and its pseudo-first-order kinetic profiles (inset panel) and (b) TOC content
577 during the PEF-like treatment under the conditions described in Fig. 4.

578 **Fig. 7.** Proposed route for SMX degradation by electrochemical Fenton-like treatments with
579 electrogenerated HClO.

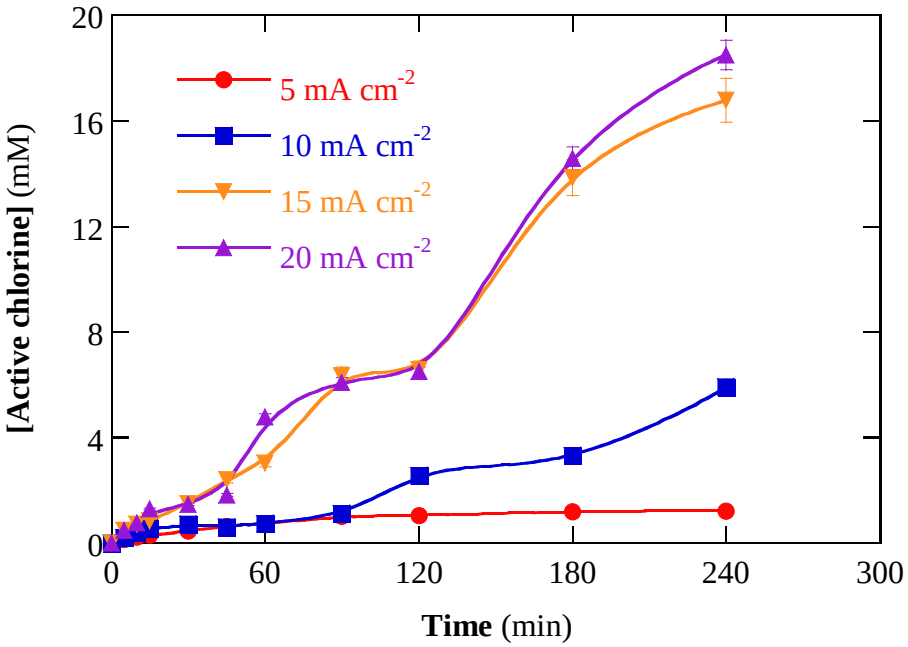
20
16
12
8
4
0
0
60
120
180
240
300
[Active chlorine] (mM)
Time (min)
5 mA cm-2
10 mA cm-2
15 mA cm-2
20 mA cm-2

Fig. 1

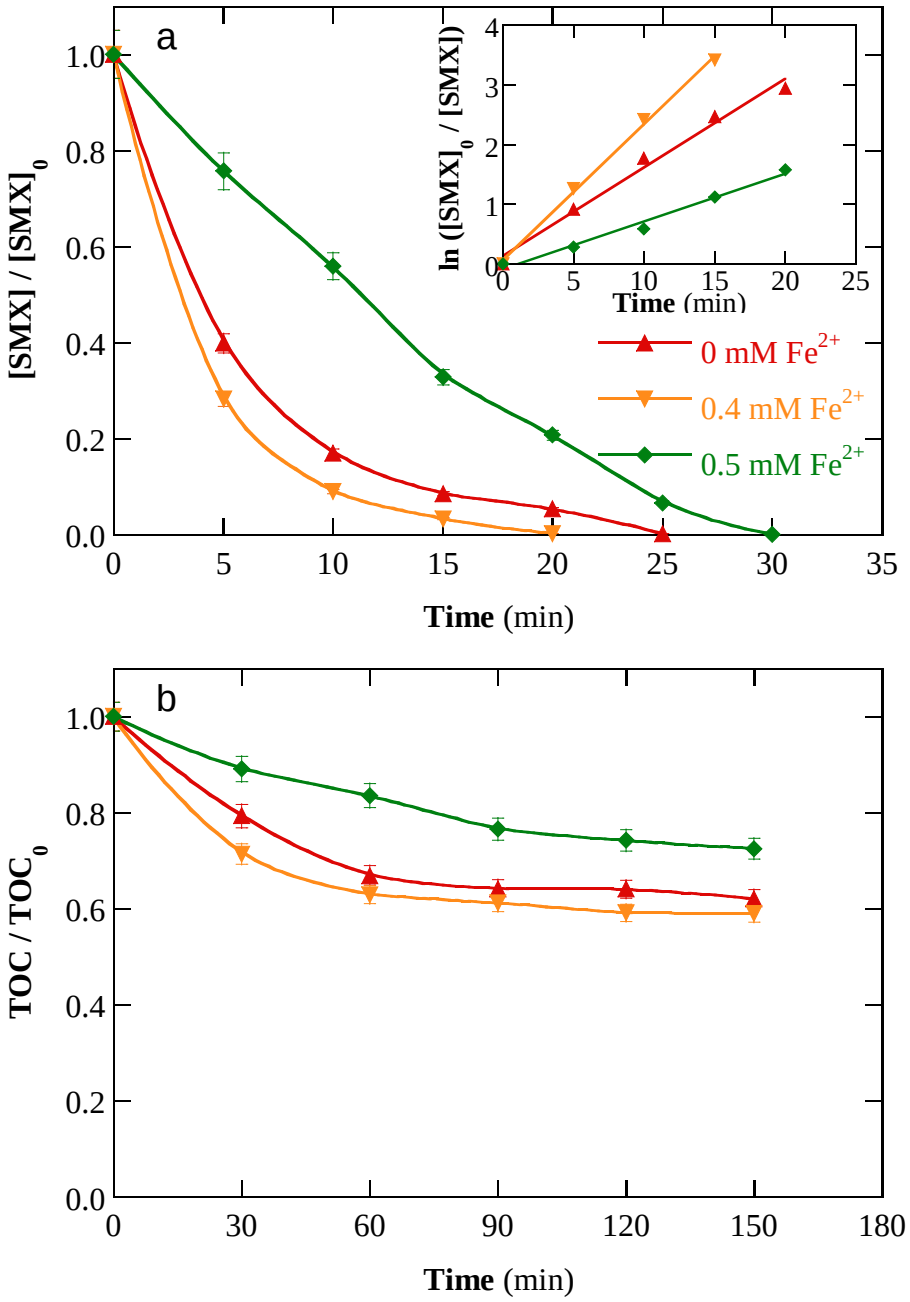
a
[SMX] / [SMX]0
Time (min)
ln ([SMX]0 / [SMX])
Time (min)
0 mM Fe2+
0.4 mM Fe2+
0.5 mM Fe2+
b
TOC / TOC0
Time (min)

Fig. 2

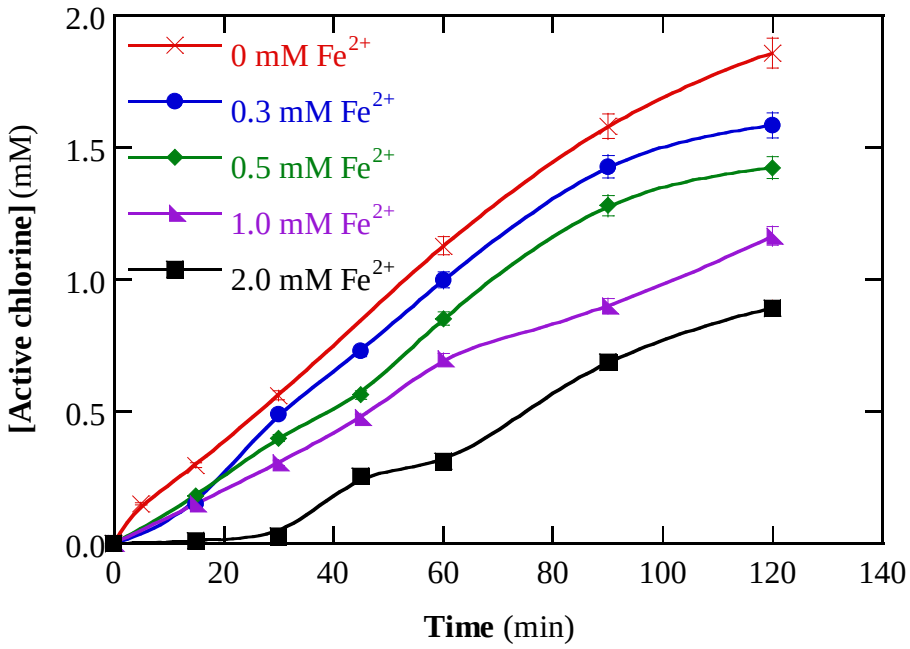
2.0
1.5
1.0
0.5
0.0
[Active chlorine] (mM)
0 mM Fe2+
0.3 mM Fe2+
0.5 mM Fe2+
1.0 mM Fe2+
2.0 mM Fe2+
0
20
40
60
80
100
120
140
Time (min)

Fig. 3

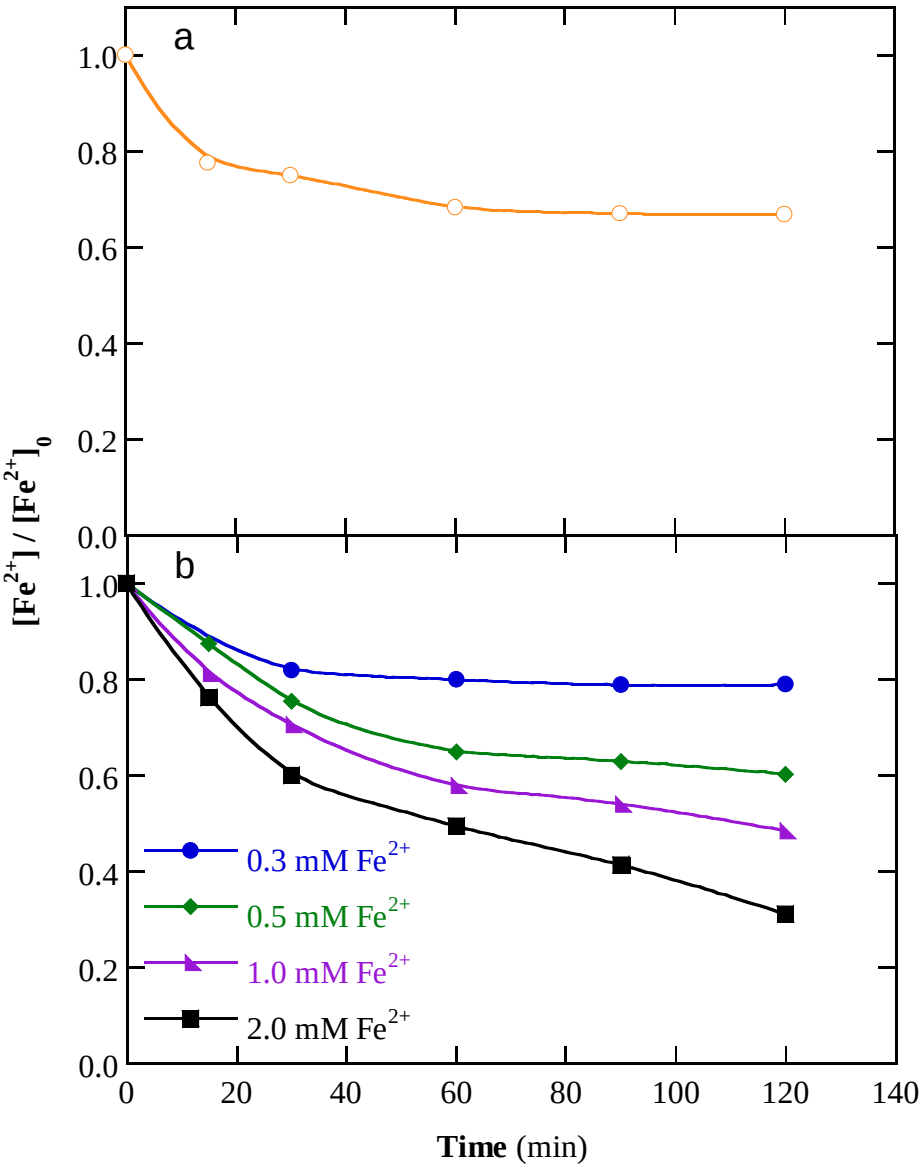
a
b
1.0
0.8
0.6
0.4
0.2
0.0
[Fe2+] / [Fe2+]0
0.3 mM Fe2+
0.5 mM Fe2+
1.0 mM Fe2+
2.0 mM Fe2+
0
20
40
60
80
100
120
140
Time (min)

Fig. 4

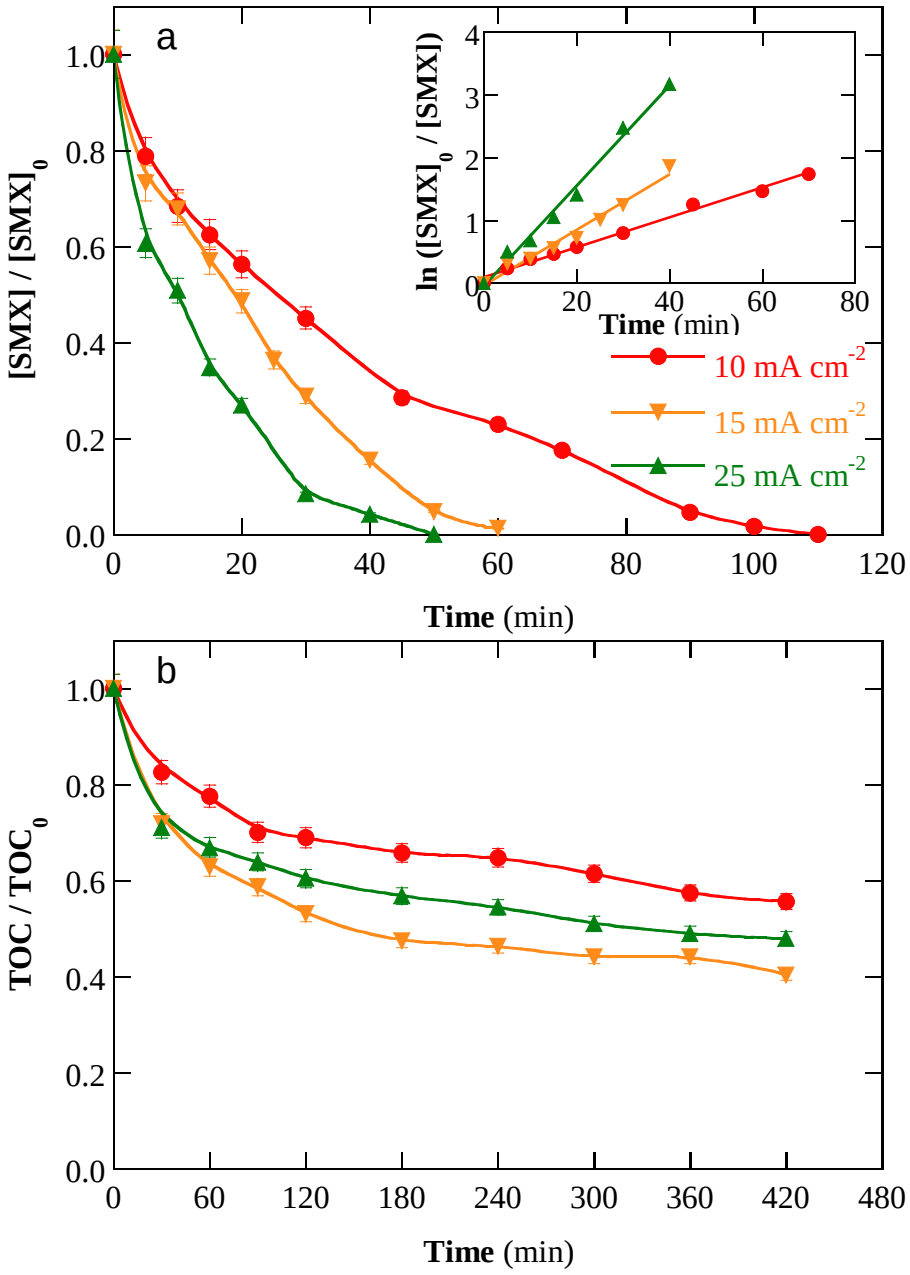
a
[SMX] / [SMX]0
Time (min)
ln ([SMX]0 / [SMX])
Time (min)
10 mA cm-2
15 mA cm-2
25 mA cm-2
b
TOC / TOC0
Time (min)

Fig. 5

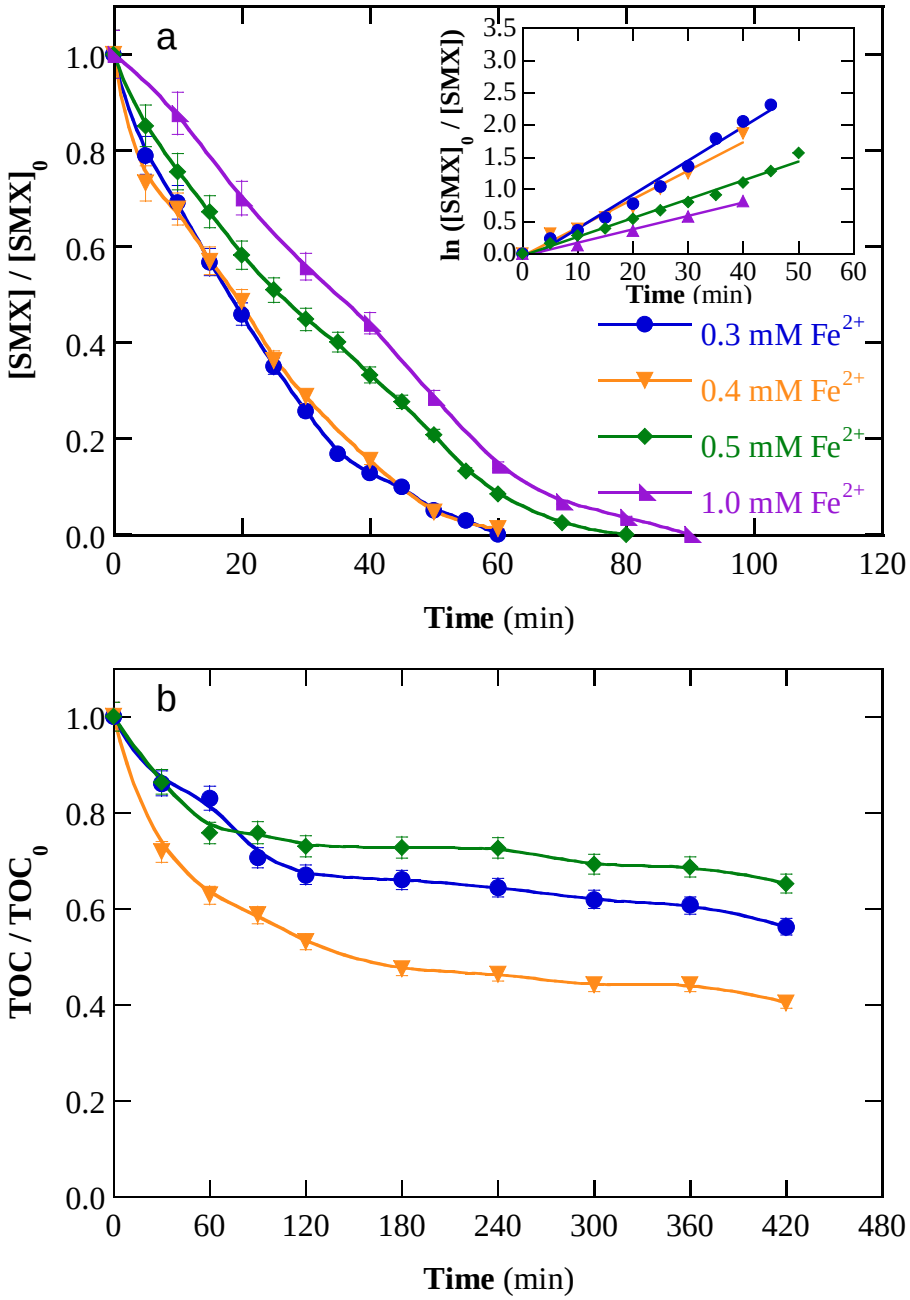
a
[SMX] / [SMX]0
Time (min)
ln ([SMX]0 / [SMX])
Time (min)
0.3 mM Fe2+
0.4 mM Fe2+
0.5 mM Fe2+
1.0 mM Fe2+
b
TOC / TOC0
Time (min)

Fig. 6

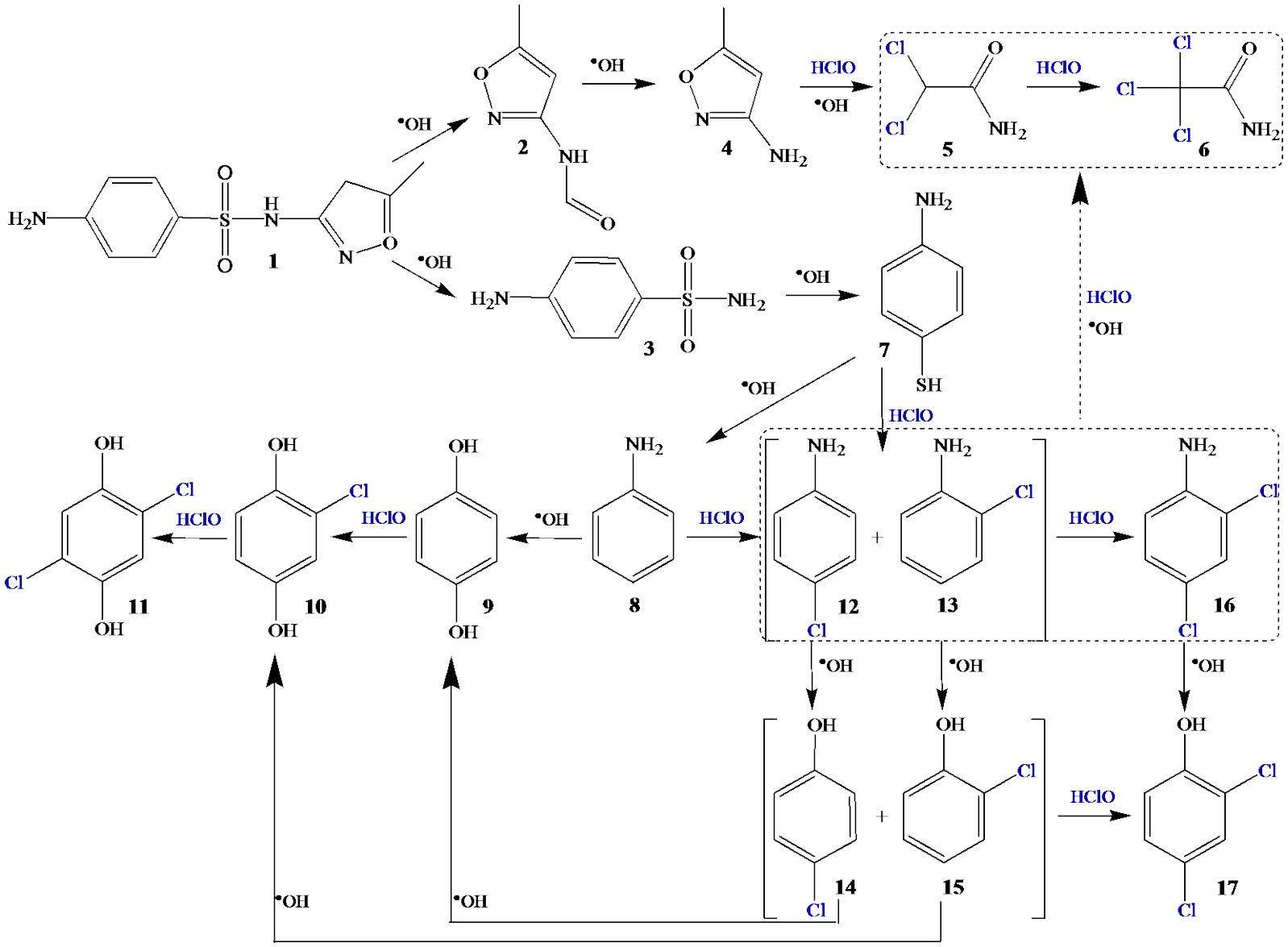

Fig. 7

Table 1

Pseudo-first-order rate constants and *R*-squared values, along with the percentage of TOC removal and energy consumption per unit TOC mass for the PEF-like treatment of 3.0 L of 0.208 mM SMX solutions at pH 3.0 and 30 ºC, using the filter-press FM01-LC reactor with an Ir-Sn-Ru oxide anode and a stainless steel cathode at liquid flow rate of 180 L h^{-1}.

Medium	j (mA cm^{-2})	$[Fe^{2+}]_0$ (mM)	k_1 (10^{-2} min^{-1})	R^2	% TOC removal	EC_{TOC} (kWh (g TOC)$^{-1}$)
25 mM Na_2SO_4 + 35 mM NaCl	15	0.4	23	0.997	41.0 [a]	1.136
		0.5	8.0	0.982	27.5 [a]	1.688
45 mM Na_2SO_4 + 15 mM NaCl	10	0.4	2.4	0.992	44.5 [b]	0.624
	15	0.3	4.7	0.982	40.8 [b]	1.059
		0.4	4.4	0.980	59.7 [b]	0.776
		0.5	2.9	0.990	34.8 [b]	1.331
		1.0	2.1	0.987	- [c]	- [c]
	25	0.4	8.0	0.990	52.1 [b]	1.887

Electrolysis time: [a] 150 min and [b] 420 min; [c] Not determined